WM-88-106

Relativistic Quark Clustering in the $\gamma\gamma \to \pi^+\pi^-$ and $\pi^0\pi^0$ reactions.

Hiroshi Ito and W. W. Buck

Department of Physics, Hampton University
Hampton, Va. 23668, U.S.A.

Franz Gross

Continuous Electron Beam Accelerator Facility
12000 Jefferson Avenue, Newport News, Va. 23606
and
Physics Department, College of William and Mary
Williamsburg, Va. 23185, U.S.A.

Abstract

Cross sections for pion pair production by photon-photon collisions are estimated near the threshold using a relativistic quark clustering model. A realistic $q\bar{q}$ wave function of the pion was determined by fitting the pion charge form factor up to $q^2 = 4 \sim 6GeV^2/c^2$, the weak decay constant and the pion charge radius. The composite structure of the pion provides a simple explanation for the energy dependence and magnitudes of $\pi^+\pi^-$ and $\pi^0\pi^0$ pair productions.

PACS numbers: 13.65.+i, 13.40.-f, 12.40.-y, 13.20.Cz.

Two pion production cross sections in photon-photon collision have been measured for the range of $\pi\pi$ invariant mass $\sqrt{s} \leq 3GeV$, and a large enhancement over the Born approximation prediction is observed[1-3] near the threshold of the $\gamma\gamma \to \pi^+\pi^-$ reaction. The Born amplitude for the neutral pion pair production $\gamma\gamma \to \pi^0\pi^0$ is zero, but data reported by the Christal Ball Collaboration[4] indicates that the cross section is not zero, but at least an order of magnitude smaller than the charged pion case, and varies slowly with energy up to the $f_2(1274)$ peak. These interesting results have stimulated theoretical speculation; Mennessier[5] introduced the direct coupling of two photons to a scalar-isoscalar meson($\epsilon(740)$), which would give a large contribution, making the $\pi^0\pi^0$ cross section approximately half of the $\pi^+\pi^-$ one. Barnes *et al*[6] keep the small $\pi^0\pi^0$ cross section and attributed the $\pi^+\pi^-$ enhancement to corrections to the Born amplitude arising from final state interactions, which they calculate from a nonrelativistic $q\bar{q}q\bar{q}$ model. Chiral perturbation theory using an effective QCD lagrangian, when applied to these reactions recently[7], gave a linear dependence of the $\pi^0\pi^0$ cross section on $\sqrt{s}$ up to $0.6 \sim 0.7GeV$.

In these approaches, including the Born calculation[8] and other older calculations[9] based on the low energy theorem, the photon is assumed to couple to the elementary field of a point-like pion. On the other hand multi-hadron production in e^+e^- colliders is now regarded as a dynamical testing ground of Quantum Chromodynamics(QCD). Here the hadron production is initiated by the coupling of the incident photons to either one or two quark pairs, and perturbative QCD has been successfully applied to the $\gamma\gamma \to \pi^+\pi^-$, K^+K^- reactions[10] in the very high energy region $\sqrt{s} > 1.5GeV$. The study of resonance processes such as the $\gamma\gamma \to \rho\rho$ has been also well developed using multi- quark models[11].

In this letter we present a calculation based on a Relativistic Quark Cluster Model(RQCM) of the $\gamma\gamma \to \pi^+\pi^-$, $\pi^0\pi^0$ cross sections near threshold. It is shown that the charge structure of the pion as a quark- antiquark($q\bar{q}$) pair provides a simple estimate for the magnitudes of both reactions. The momentum distributions of confined quarks, especially of the soft part of the wave function, is properly taken into account by choosing a Bethe-Salpeter amplitude of the $q\bar{q}$ bound system which gives the right sizes for the pion charge form factor, charge radius r_π, and weak decay constant f_π. Since the $\gamma\gamma \to \pi\pi$ reaction is the simplest multi-hadron process, and the photon probes the intrinsic structure of the pion,

this process is well suited to a test of the RQCM, in which both the relativistic nature of quarks and the relativistic motion of composite hadrons are expected to be well described. We plan eventually to use this model to estimate the size of quark effects in the medium energy region of nuclear physics.

We start with the charge structure of the transition amplitudes $M^a_{\gamma\gamma\to\pi\pi'}$ and $M^b_{\gamma\gamma\to\pi\pi'}$ illustrated by the Feynmann diagrams of Fig. 1. Assuming SU(2) flavor symmetry for light quarks, $m_u = m_d$, permits a factor depending only on the charge to be separated from the dynamical part, giving

$$M^a_{\gamma\gamma\to\pi\pi'} = Tr\left[\Phi^\pi e_q \Phi^{\pi'} e_q\right] \otimes \int \frac{d^4k}{(2\pi)^4} Tr\{g_1\}, \tag{1a}$$

$$M^b_{\gamma\gamma\to\pi\pi'} = Tr\left[\Phi^\pi \Phi^{\pi'} e_q e_q\right] \otimes \int \frac{d^4k}{(2\pi)^4} Tr\{g_2\} + Tr\{g_2(\epsilon_a, q_a \leftrightarrow \epsilon_b, q_b)\}, \tag{1b}$$

where

$$g_1 = \not\epsilon_a S(k - q_a)\Gamma_b S(k + p_b - q_a)\not\epsilon_b S(k - p_a)\Gamma_a S(k),$$

and

$$g_2 = \not\epsilon_a S(k - q_a)\not\epsilon_b S(k - p_b - p_a)\Gamma_b S(k - p_a)\Gamma_a S(k).$$

Here $\Gamma_a \equiv \Gamma(p_a - k, k)$ is the Bethe-Salpeter vertex function of the pion(a), where k and $p_a - k$ are the momentum of the quark and antiquark, respectively. $S(k)$ is the propagator of quark with the four momentum k and mass m_q, and ϵ_a, ϵ_b are the polarization vectors of incident photons. The 2×2 matrices e_q, Φ^0, Φ^+ and Φ^- are the quark charge operator and flavor density matrices of π^0, π^+ and of π^- mesons.

$$e_q = \begin{bmatrix} 2e/3, & 0 \\ 0, & -e/3 \end{bmatrix}, \ \Phi^0 = \begin{bmatrix} 1/\sqrt{2}, & 0 \\ 0, & -1/\sqrt{2} \end{bmatrix}, \ \Phi^+ = \begin{bmatrix} 0, & 1 \\ 0, & 0 \end{bmatrix}, \ \Phi^- = \begin{bmatrix} 0, & 0 \\ 1, & 0 \end{bmatrix}.$$

The γ_5 and γ^μ matrices in the respective pion(Γ_b) and photon($\not{\epsilon}_b$) vertices are in a different order in g_1 and g_2, and this gives opposite signs in the dynamical part of loop integrals in the Eqs.(1a,b), where each magnitude depends upon the quark mass and details of the momentum distributions. The traces of the charge operators are $Tr[\Phi^0\Phi^0 e_q e_q] = Tr[\Phi^0 e_q \Phi^0 e_q] = \frac{5e^2}{18}$ for the $\gamma\gamma \to \pi^0\pi^0$ case, and this results in a strong cancellation of the amplitudes $M^a_{\gamma\gamma\to\pi\pi'}$ and $M^b_{\gamma\gamma\to\pi\pi'}$ yielding the very small cross section. On the contrary, in the charged pion case $Tr[\Phi^+\Phi^- e_q e_q] = \frac{8e^2}{18}$, $Tr[\Phi^+ e_q \Phi^- e_q] = \frac{-4e^2}{18}$, $Tr[\Phi^-\Phi^+ e_q e_q] = \frac{2e^2}{18}$ and $Tr[\Phi^- e_q \Phi^+ e_q] = \frac{-4e^2}{18}$, which results in the large coherent sum of the total amplitude. Therefore the details of the hadron structure will be magnified after computing all the 6 diagrams, i.e. $M^a_{\gamma\gamma\to\pi\pi'} + M^b_{\gamma\gamma\to\pi\pi'}$ and their $p_a \leftrightarrow p_b$ exchange.

We have undertaken an empirical analysis[12] of the pion structure based upon the Bethe-Salpeter formalism. The pseudo-scalar $q\bar{q}$ bound state wave function will be expressed by the Dirac gamma matrices γ_5 and $\gamma_5\not{p}$, where p is the four momentum of pion, and we take a mixed form of the wave function

$$\Psi(p-k,k) = \frac{N}{D(K^2)}\{(1-\eta)\gamma^5 + \eta\gamma^5\frac{\not{p}}{M}\} \tag{2}$$

Here N is a normalization constant given by the charge normalization and M is a constant with a dimension of mass($Mc^2 = 138.MeV$ is used). $D(K^2)$ describes the momentum distribution of $q\bar{q}$ pair as a function of their relative momentum $K = k - \frac{p}{2}$. In order to have a finite value of the loop integral in the calculation of the pion decay constant, which is typically given by $f_\pi \sim \int d^4k\Psi(p-k,k)$, $D(K^2)$ has to behave like $\sim K^n, n \geq 6$. We use the following simple product of monopole functions, with the parameters Λ_1, Λ_2 and Λ_3 roughly estimating the scales of soft and hard regions.

$$D(K^2) = [K^2 - \Lambda_1^2][K^2 - \Lambda_2^2][K^2 - \Lambda_3^2]. \tag{3}$$

The BS wave function(Ψ) and the vertex function(Γ) are related by $\Psi(p-k,k) = S(k-p)\,\Gamma(p-k,k)S(k)$, and we have evaluated the pion charge radius(r_π) , weak decay constant (f_π) and charge form factor ($F_\pi(q^2)$) by using the above vertex function in their loop diagrams. The details are given in Ref. 12. The gluon exchange is not explicitly included here assuming that our phenomenology will cover this effect, or alternatively, that our wave function fits only the soft contribution, and that the hard gluon correction is small and can be estimated later for all the observables. Four parameters Λ_1, Λ_2, Λ_3 and η are adjusted to minimize the χ^2 distribution for 10 data; r_π,f_π, and 8 data points from the charge form factor shown by the solid circles of Fig. 2. The result of this analysis is given in Table 1 and Fig. 2. Early in this analysis we treated the quark mass as one of the adjustable parameters to minimize the χ^2, but the result was very insensitive to the value of m_q since f_π depends on m_q only through the normalization constant N, which has a very slow dependence on the quark mass. Here we take $m_q = 350MeV$, equal to the constituent quark mass. (With the choice of $m_q = 250MeV$ we found $\chi^2 = 0.48/Data\ point$, and for $m_q = 450MeV$, $\chi^2 = 0.49/Data\ point$, without significant change of other parameters given in Table 1).

Fig. 3 presents the results of the two pion production cross sections calculated with the parameters given in the Table 1. In the present approach a possible way to study the sensitivity to soft processes in QCD is to change the confinment scale. For this test we made a reference wave function of a smaller pion by introducing a smaller value of $r_\pi \sim 0.4 \pm 0.05 fm$ in the analysis, and we found $\Lambda_1 = 1.46 fm^{-1}, \Lambda_2 = 3.3 fm^{-1}, \Lambda_3 = 3.7 fm^{-1}$, $\eta = 0.09$, $r_\pi = 0.42 fm$, and $f_\pi = 92MeV$. The results with this smaller pion are also shown. Our conclusions are,

(a)$\gamma\gamma \to \pi^+\pi^-$: The integrated cross section, shown in Fig. 3a, is compared with the experiments reported by Refs 1 and 3 and with the prediction by the Born approximation. Our result agrees with these measurments except for the dip around $\sqrt{s} = 0.45 \sim 0.5GeV$ observed by Ref. 3. The result with the reference wave function of the smaller pion shows about $\sim$ 20% reduction from the one predicted with our wave function. The quark mass dependence is estimated using the parameters of Table 1. With the value $m_q = 450MeV$, the cross section is 5% smaller at $\sqrt{s} = 0.34GeV$, and 4% smaller at $\sqrt{s} = 0.44GeV$.

(b)$\gamma\gamma \to \pi^0\pi^0$: The integrated cross section for $|cos\theta| < 0.8$ is compared with the experimental data[4] in Fig. 3b. Our result, shown by the solid line, predicts the right magnitude and energy dependence. We observe the strong sensitivity to the size of pion; the smaller pion($r_\pi = 0.42fm$) reduces the cross section about a factor $\sim \frac{1}{3}$ or more. The quark mass dependence is found to be $\sigma(m_q = 450MeV)/\sigma(m_q = 350MeV) = 1.19$ at $\sqrt{s} = 0.34GeV$ and 1.23 at $\sqrt{s} = 0.44GeV$. Note that the cross section is rising as $\sqrt{s} \to\sim 4\Lambda_1$, the location of the cuts resulting from the structure of the wave function.

We also calculated[12] the two photon decay width of a neutral pion $\Gamma_{\pi^o\to 2\gamma}(7.57 \pm 0.3eV$[14]) to test the pion wave function of Table 1. The simple evaluation of the triangular diagrams gives $\Gamma_{\pi^o\to 2\gamma} = 1.17eV$ for $m_q = 350MeV$, and $1.25(0.97)eV$ for $m_q = 250(450)MeV$.

The calculation of the amplitude $M^b_{\gamma\gamma\to\pi\pi'}$ involves a 4 dimensional integral of the Feynman parameters, such as $\int dx_1 \int dx_2 \int dx_3 \int dx_4 \delta(x_1+x_2+x_3+x_4-1) f(x_1,x_2,x_3,x_4)$, and we performed this integral by the Monte Carlo method on the surface of a 4-dimensional hypersphere.

In summary, we observe that treatment of the pion as a relativistic quark-antiquark system provides a simple estimate for both $\gamma\gamma \to \pi^+\pi^-, \pi^0\pi^0$ reactions in rough agreement with existing data. The interplay of the pion charge structure and the momentum distribution of the constituent quarks is crucial to the quantitative explanation of the energy dependence of the cross sections. Theoretical predictions of the cross sections, especially for π^0 pair production, are very sensitive to the confinement size, considered to be the size of the pion, rather than the constituent quark mass. A question remains about possible corrections from final state interactions such as the coupled channel process $\gamma\gamma \to \pi^+\pi^- \to \pi^0\pi^0$. The corrections to the Born amplitudes from these processes have been well studied[5,6]. This effect can be included in the RQCM and would change the present estimate. Unlike the conventional approach to photo-hadron production, however, the hadronization and the mutual hadronic interaction are not clearly separated in QCD. Both processes would happen in the dynamical evolution of hadronization. At this level the dynamical calculation with an exact algorithm, such as the lattice simulation of hadron structure[15], will provide a more systematic approach. In addition, the rule of the axial

anomaly[16] sould be developed in the context[17,18] of quark confinement. We hope the present phenomenological approach provides a useful guide to further study.

The work of H.I was supported by NSF grant RII-8704038, that of W.W.B was supported by NASA grant NAG-1-447 and RII-8704038, and that of F.G was supported in part by the Departmant of Energy grant number DE-FG05-88ER40435. H.I and W.W.B would like to thank the Continuous Electron Beam Accelerator Facility(CEBAF) for the hospitality and for the computer facilities. H.I is indebted to Dr. G. P. Lepage for his useful comment and for offering the computer code VEGA. The very helpful advice by Dr. C. Carlson is greatly appreciated.

References

1. A. Courau *et al.*(DM1 Collab.), Nucl. Phys. **B271**, 1 (1986).
2. Z. Ajaltouni *et al.*(DM2 Collab.), Contrib. VIIth Intern. Workshop on Photon-photon collisions, Paris, April 1986.
3. Ch. Berger *et al.*(PLUTO Collab.), Z. Phys. **C26**, 199 (1984).
4. H. Marsiske *et al.*(Crystal Ball Collab.), Contrib. 23rd Intern. Workshop on High energy physics, Berkeley, July 1986, cited by S. J. Brodsky SLAC-PUB-4648.
5. G. Mennessier, Z. Phys. **C16**, 241 (1983).
6. T. Barnes, K. Dooley and N. Isgur, Phys. Lett. **B183**, 210 (1987).
7. J. Bijnens and F. Cornet, Nucl. Phys. **B296**, 557 (1988).
8. S. J. Brodsky, T. Kinoshita and H. Terazawa, Phys. Rev. **D4**, 1532 (1971).
9. H. Terazawa, Phys. Rev. Lett. **26**, 1207 (1971), R. L. Goble and J. L. Rosner, Phys. Rev. **D5**, 2345 (1972).
10. S. J. Brodsky and G. P. Lepage, Phys. Rev. **D24**, 1808 (1981), S. J. Brodsky, G. Kõpp and P. M. Zerwas, Phys. Rev. Lett. **58**, 443 (1987).
11. B. A. Li and K. F. Liu, Phys. Rev. Lett. **51**, 1510 (1983).
12. H. Ito, W. W. Buck and F. Gross, in preparation for submit, or in Proceedings of Workshop "Nuclear and Particle physics on the Light cone", Los Alamos, July 1988(to be published).
13. C. J. Bebek *et al*, Phys. Rev. **D17**, 1693 (1978).
14. M. Aguilar-Benitez *et al.*(Particle Data Group), Phys. Lett. **170B**, 1 (1986).
15. S. Huang, J. W. Negele and J. Polonyi, Nucl. Phys. **B307**, 669 (1988), and references therein. G. A. Miller, University of Washington preprint #40427-09-N8.
16. S. L. Adler, Phys. Rev. **177**, 2426 1969). J. S. Bell and R. Jackiw, Nuovo Cim. **60A**, 47 (1969).
17. K. Fujikawa, Phys. Rev. Lett. **42**, 1195 (1979).
18. L. H. Karsten and J. Smit, Nucl. Phys. **B183**, 103 (1981).

Figure captions

Fig. 1

The Feynmann diagrams for (a)the quark exchange amplitude $M^a_{\gamma\gamma\to\pi\pi'}$ and (b)the quark loop amplitude $M^b_{\gamma\gamma\to\pi\pi'}$. The wavy, solid and double solid lines stand for photon, quark and pion respectively. The four momenta of photon $a(b)$ and pion $a(b)$ are $q_a(q_b)$ and $p_a(p_b)$, respectively.

Fig. 2

The charge form factor of the pion. The solid line is the fit resulting from the parameters in Table 1. The experimental data are taken form Ref. 13.

Fig. 3

(a)The integrated cross section of $\gamma\gamma \to \pi^+\pi^-$, where the solid line is our result using the parameters in Table 1, and the dashed line is for the the reference wave function of a small pion. The the dotted-dash line shows the Born amplitude prediction. The experimental data are from Ref. 1 (solid circles) and from Ref.3 (diamonds). (b)The integrated cross section($| cos\theta | < 0.8$) of $\gamma\gamma \to \pi^0\pi^0$. The meaning of lines is the same as in (a). The experimental data are taken from Ref. 4.

Table captions

Table 1

The parameters of the pion wave function Eq(2) and the static observables which result from the χ^2 fitting. The numbers in the parentheses are the experimental values.

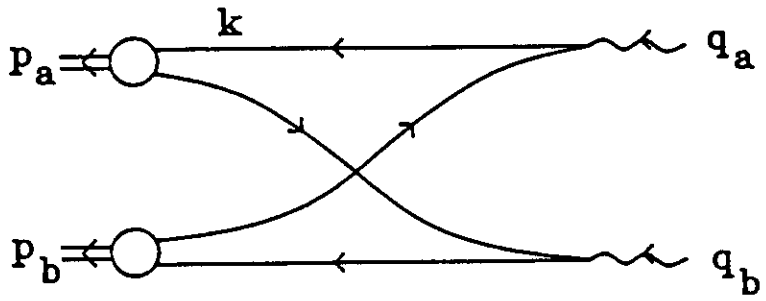

(a)

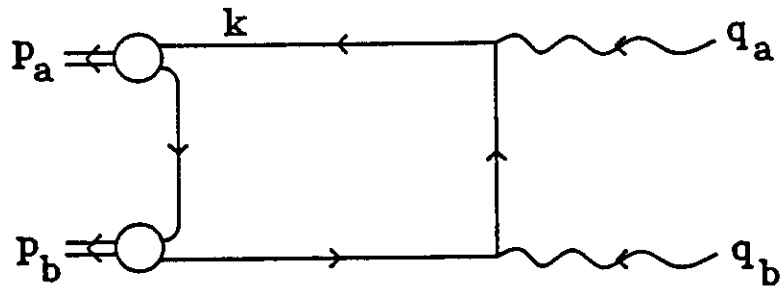

+

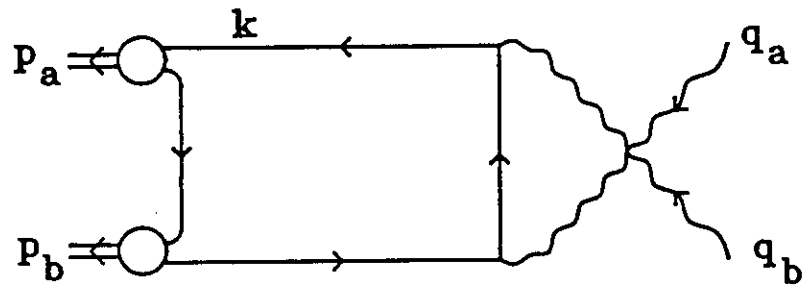

(b)

Fig. 1

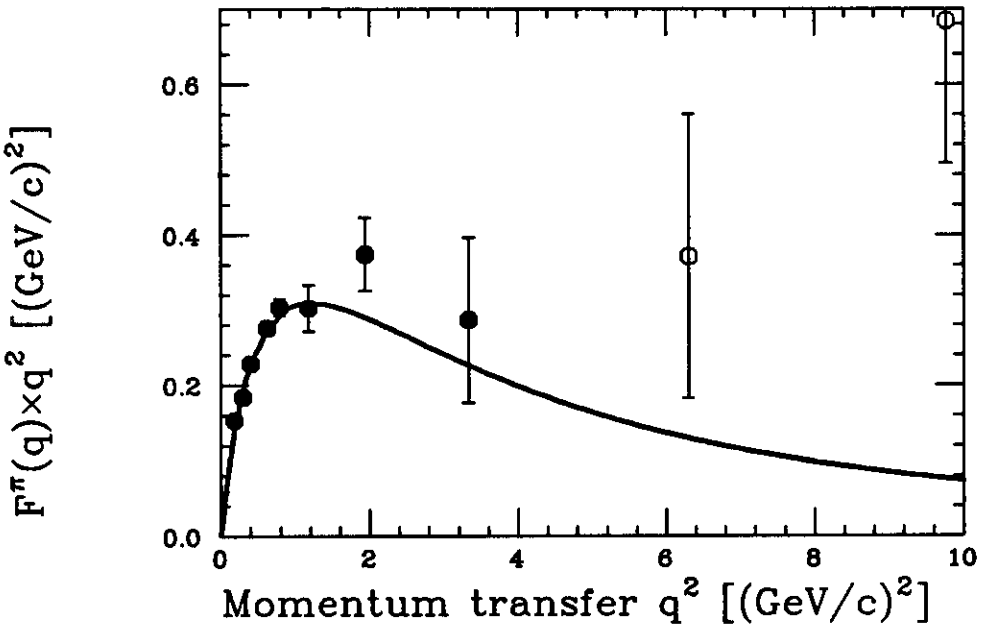
$F^{\pi}(q)\times q^2$ [(GeV/c)^2]
0.0
0.2
0.4
0.6
0
2
4
6
8
10
Momentum transfer q^2 [(GeV/c)^2]

Fig. 2

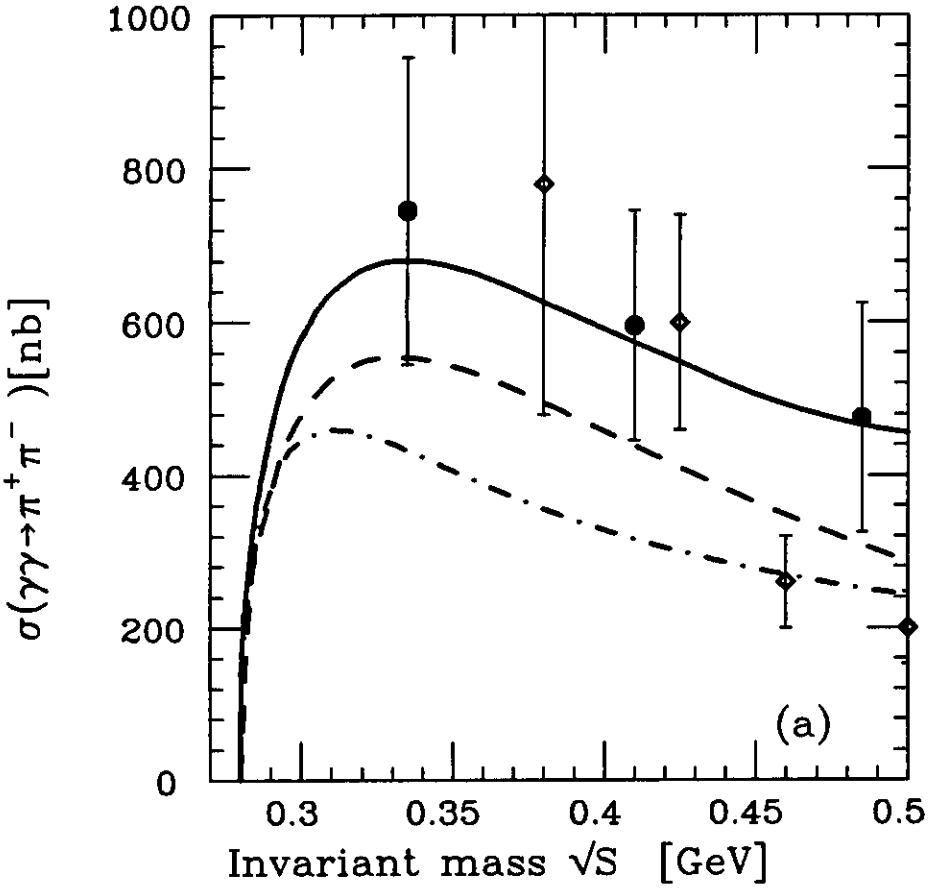
1000
800
600
400
200
0
$\sigma(\gamma\gamma\to\pi^+\pi^-)$[nb]
(a)
0.3
0.35
0.4
0.45
0.5
Invariant mass √S [GeV]

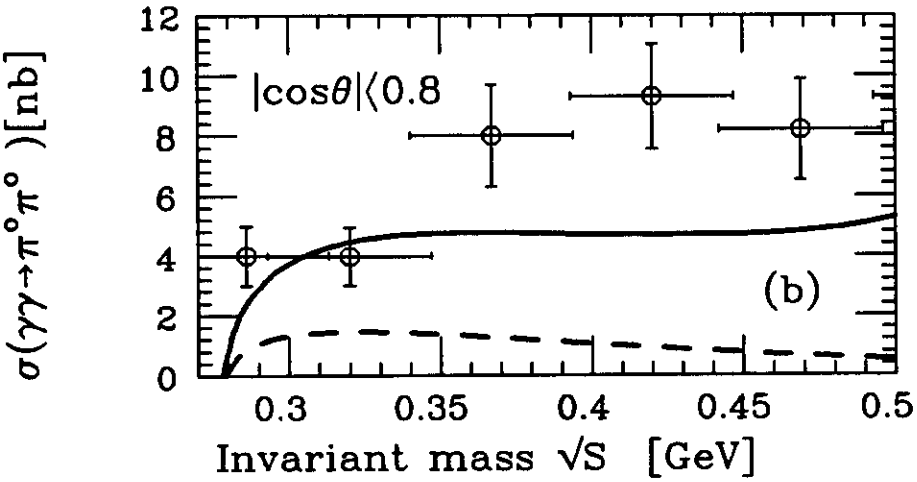
12
10
8
6
4
2
0
$\sigma(\gamma\gamma\to\pi^0\pi^0)$[nb]
|cosθ|<0.8
(b)
0.3
0.35
0.4
0.45
0.5
Invariant mass √S [GeV]

Fig. 3

$\Lambda_1[fm^{-1}]$	$\Lambda_2[fm^{-1}]$	$\Lambda_3[fm^{-1}]$	η	$\chi^2/(DataPt.)$	$r_\pi[fm]$	$f_\pi[MeV]$	$m_q c^2[MeV]$
0.694	3.412	3.763	0.078	0.49	0.640 (0.663±0.023)	93.1 (93.)	350.0

Table 1

PRINTING SEQUENCE SHEET
5ND NPPSO 5603/30
SHEET 1

CODES: HT – HALFTONE
CC – CAMERA COPY
NF – NEG. FURNISHED
SC – SELF COVER
FO – FOLD-OUTS
IN – INSERTS (DIVIDERS ETC.)
SI – STRIP-IN
CS – COVER SEPARATE

LINE	FACE PAGE NO.	FACE CODE	LINE	BACK PAGE NO.	BACK CODE	LINE	FACE PAGE NO.	FACE CODE	LINE	BACK PAGE NO.	BACK CODE
1	overlay for cover		2	blank		61			62		
3	title pg		4	2		63			64		
5	3		6	4		65			66		
7	5		8	6		67			68		
9	7		10	8		69			70		
11	9		12	10		71			72		
13	Fig 1		14	Fig 2		73			74		
15	Fig 3		16	Table 1		75			76		
17			18			77			78		
19			20			79			80		
21			22			81			82		
23			24			83			84		
25			26			85			86		
27			28			87			88		
29			30			89			90		
31			32			91			92		
33			34			93			94		
35			36			95			96		
37			38			97			98		
39			40			99			100		
41			42			101			102		
43			44			103			104		
45			46			105			106		
47			48			107			108		
49			50			109			110		
51			52			111			112		
53			54			113			114		
55			56			115			116		
57			58			117			118		
59			60			119			120		

RECAP

Printed Pages	Blank Pages	Total Pages	Total Pages (Code Std.)	Halftones	Camera Copy	Neg. Furnished

Fold-Outs 17"	22"	35"	45"	56"	60"	Over 60"	Inserts (Dividers, etc.)	Sequence Sheets
								_____ of _____